ELSEVIER

25 August 1995

Chemical Physics Letters 242 (1995) 427–434

CHEMICAL
PHYSICS
LETTERS

LIF detection of IO and the rate coefficients for I + O_3 and IO + NO reactions

Andrew A. Turnipseed [a,b], Mary K. Gilles [a,b], James B. Burkholder [a,b],
A.R. Ravishankara [a,b,*,1]

[a] National Oceanic and Atmospheric Administration, Aeronomy Laboratory, 325 Broadway, Boulder, CO 80303, USA
[b] Cooperative Institute for Research in Environmental Studies, University of Colorado, Boulder, CO 80309, USA

Received 2 May 1995; in final form 30 June 1995

Abstract

Laser induced fluorescence (LIF) from the (0, 0), (2, 0), (3, 0), and (2, 1) bands of the $A^2\Pi_{3/2} \leftarrow X\,^2\Pi_{3/2}$ system of IO was detected. Using LIF detection of IO, the rate coefficients for $I + O_3 \rightarrow IO + O_2$ (k_1) and $IO + NO \rightarrow I + NO_2$ (k_2) reactions were measured between 240 and 370 K to be $k_1(T) = (2.3 \pm 0.7) \times 10^{-11} \exp[-(860 \pm 100)/T]$ and $k_2(T) = (1.02 \pm 0.31) \times 10^{-11} \exp[(185 \pm 70)/T]$ cm^3 molecule^{-1} s^{-1}.

1. Introduction

The presence of iodine compounds in the Earth's biosphere and oceans, as well as in the atmosphere, has been recorded for quite some time [1–4]. The role of iodine in the chemistry of the atmosphere has been the subject of speculation and investigations in the past few decades [5–7]. Specifically, the role of gas phase iodine chemistry in the marine boundary layer of the atmosphere and its effect on the abundances of ozone and other chemicals have been investigated [8,9]. Iodine containing compounds have been shown to be present in the Arctic springtime troposphere [10]. Very recently, Solomon et al. [11] speculated that catalytic reactions of the IO radical could be, at least partly, responsible for the depletion of lower stratospheric O_3 and the sudden episodic ozone disappearance in the Arctic troposphere during the springtime. Evaluation of this hypothesis requires kinetic, photochemical, and heterogeneous reaction rate data. Two reactions that play important roles in the chemistry of iodine in the atmosphere are:

$$I + O_3 \rightarrow IO + O_2, \qquad (1)$$

$$IO + NO \rightarrow I + NO_2. \qquad (2)$$

Reaction (1) is a key step in the iodine catalyzed O_3 destruction cycles and reaction (2) links NO_x chemistry with that of iodine and affects the partitioning between I and IO in the atmosphere.

One of the major difficulties in studying reactions of IO is the lack of a suitable sensitive and non-intrusive detection technique that can be employed at atmospheric pressures, in very small volumes, and in the absence of surface effects. Laser induced fluorescence (LIF) is one such common and convenient detection method. However, there are contradictory reports on the feasibility of inducing fluorescence in the $A^2\Pi_{3/2} \leftarrow X\,^2\Pi_{3/2}$ system of IO. Watson et al.

---

[*] Corresponding author. Correspondence should be addressed to the National Oceanic and Atmospheric Administration.

[1] Also affiliated with the Department of Chemistry and Biochemistry, University of Colorado, Boulder, CO 80309, USA.

SSDI 0009-2614(95)00774-1

[12] and Kwong and Tse [13] were unable to observe LIF; however, both Inoue et al. [14] and Bekooy et al. [15] observed fluorescence. Since LIF could be an extremely useful scheme for detection of IO in the atmosphere and laboratory, we have investigated this process.

A concerted effort has been initiated in our laboratory to measure the various kinetic and photochemical parameters needed to evaluate the role of iodine in the atmosphere. Here, we report on the LIF detection of IO and the kinetics of reactions (1) and (2). These reactions were studied because they are atmospherically important, involve only one unstable radical reactant, and have been studied before using other methods [16,17]. Reactions involving one unstable radical are easier to study and previous kinetics data allows us to test our new experimental method involving LIF detection of IO.

2. Experiments and results

The apparatus used in this study has been used routinely in our laboratory to produce OH [18], CH_3S [19], and CF_3O [20] radicals via pulsed laser photolysis and to detect them via pulsed LIF. We will not describe this apparatus here but provide only the information necessary to understand the LIF detection of IO and kinetics of reactions (1) and (2).

2.1. LIF detection of IO

IO was generated by reactions (1), (3), (4) or (5) in a slow flow of an excess of He and/or N_2,

$$O(^3P) + I_2 \rightarrow IO + I, \tag{3}$$

$$O(^3P) + CH_3I \rightarrow IO + CH_3, \tag{4a}$$

$$\rightarrow \text{products}, \tag{4b}$$

$$O(^3P) + CF_3I \rightarrow IO + CF_3, \tag{5a}$$

$$\rightarrow \text{products}. \tag{5b}$$

Reaction (3) is known to be rapid [16,17] and rate coefficients for reactions (4) and (5) have been found in our laboratory to be high. These results will be reported elsewhere [21]. Ground state O atoms, $O(^3P)$, were produced by pulsed excimer laser photolysis of O_3 (at 248 nm) or of N_2O (at 193 nm) in N_2. Photolytically produced $O(^1D)$ was rapidly quenched to $O(^3P)$ by N_2. I atoms for reaction (1) were generated by 351 nm photolysis of CH_2I_2. Use of multiple IO production methods gives us confidence that we were detecting IO and only IO. The excitation wavelength in the range of 425 to 476 nm was generated by a XeCl-excimer laser pumped dye laser (coumarin 47 and stilbene 3 dyes). The line width of the dye laser output was 0.0025 nm and the pulse width was ≈ 10 ns. The photolysis and excitation lasers were propagated perpendicular to each other. The photolysis laser was also passed through the reactor orthogonal to the direction of the gas flow to ensure that a fresh gas mixture was photolyzed with each laser pulse. Fluorescence was collected orthogonal to the two laser beams, passed through a glass filter (either $\lambda > 475$ nm or $\lambda > 495$ nm) to discriminate against scattered light from the probe laser, and then imaged onto a photomultiplier tube (PMT). The PMT output was either fed into a gated charge integrator or to a fast wave form digitizer. This data was transferred to a microcomputer for analysis.

The excitation spectrum of IO was recorded by collecting the light transmitted through the cut-off filter while scanning the excitation wavelength. Since the fluorescence lifetime was close to (or shorter than) the pulse width of the excitation laser, we could not discriminate in time between the fluorescence from IO and scattered laser light from the excitation laser; both were collected. The scattered laser light induces fluorescence from the cut-off filter and/or the cell walls. This light detected by the filter/PMT combination was found to be very short-lived. In a separate experiment, only scattered probe laser light was collected by blocking the photolysis laser (i.e. not making IO). This background was subtracted from the total signal to obtain the LIF signal. The background was typically < 10% of the LIF signal at the peak.

Fig. 1 shows the observed excitation spectra from the (2, 0), (3, 0), (0, 0), and (2, 1) bands of the A–X system in IO. The spectra have not been corrected for variations in the probe fluence, transmission of the filter or the response of the PMT at various wavelengths. The positions of the band heads are in reasonable agreement with literature values [22] within the accuracy of our wavelength calibration

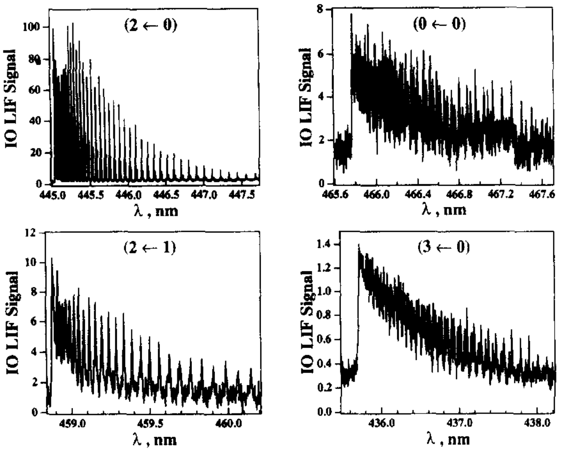

Fig. 1. Laser excitation spectra of IO $A^2\Pi_{3/2} \leftarrow X^2\Pi_{3/2}$, where the vibrational transitions are denoted $(v' \leftarrow v'')$ in the figure. The excitation laser line width was 0.0025 nm. The spectra are scaled to the intensity of the (2, 0) bandhead to show the relative intensity observed. Wavelengths are in air at 298 K and 630 Torr.

(±0.2 nm). Previous studies have observed fluorescence from the (2, 0) [14,15], (0, 0) [14], (2, 1) [15], and (2, 2) [15] bands. To our knowledge fluorescence from the (3, 0) band has not been reported previously. Since we did not obtain the dispersed fluorescence from any of these bands, the exact wavelengths of the fluorescence is not clear.

Qualitative observations about the LIF from IO are: (a) The fluorescence from the (2, 0) band was very strong. It was easily seen on an oscilloscope without signal averaging. The detection limit for IO at the (2, 0) band head was typically $\approx 1 \times 10^9$ molecule cm^{-3} for a $S/N = 1$ and averaging 100 laser shots. (b) The (2, 0) band was the most intense; the (3, 0) band was ≈ 100 times weaker and the (0, 0) band ≈ 15 times weaker than the (2, 0) band. (c) All sources of IO yielded the same excitation spectra. (d) Changes in the delay between the photolysis and the probe laser changed the magnitude of the signal at all wavelengths but not the relative intensities of various peaks.

By photolyzing a mixture of the CH_2I_2/O_3 system in 100 Torr of N_2 at 351 nm, transitions arising from the $v'' = 1$ state were observed. The intensity of the (2, 1) band was 10 times weaker than that from the (2, 0) band. When corrected for the differences in the Franck–Condon factors [23] between these two transitions and the probe laser fluences, the intensity was ≈ 4% of the (2, 0) transition. This is in agreement with the expected population of the $v'' = 1$ level for a Boltzmann population at 298 K. Fluorescence from the (2, 2) band has been reported by Bekooy et al. [15], but we were unable to detect fluorescence from this band. This was due in part to the low population of the $v'' = 2$ state at 298 K (≈ 0.2%, assuming a Boltzmann distribution), compared to the high temperatures (≈ 600 K) in the study of Bekooy et al., and in part because the (2, 2) band position (at ≈ 473 nm) lies on the edge of the tuning range for our dye. Hence, a sufficient laser energy was not available. Also, attempts to detect fluorescence from the (4, 0), (1, 0), and (1, 1) bands were unsuccessful.

Using a fast transient digitizer, the lifetime of $IO(A^2\Pi)$ was observed to be < 20 ns, the time constant of our detection system. This short lifetime agrees with the value of < 10 ns previous reported by Inoue et al. [14]. This short lifetime is, however, sufficient to produce easily detectable amounts of fluorescence from IO. It also indicates that the LIF detection sensitivity will not be reduced at higher pressures because electronic collisional quenching cannot compete with the dissociative lifetime of IO $(A^2\Pi)$.

While Inoue et al. reported difficulties with several methods of IO production [14], we did not encounter them. For example, we had no difficulty in producing IO by photolyzing a mixture of CF_3I/N_2O at 193 nm and saw no interference from IF fluorescence. Similarly, we could easily produce IO from a mixture of O_3/CH_3I and O_3/CF_3I via reactions (4) and (5). It should be noted that we always operated with low concentrations of IO ($< 4 \times 10^{12}$ molecule cm^{-3}) to minimize the self reaction of IO and limit the production of aerosols. Use of low [IO], along with the use of He or N_2 flush gases on the entrance and exit windows of the lasers, resulted in little or no solid deposits on the windows. The unsuccessful attempts of Kwong and Tse [13] were likely due to high concentrations of $O(^3P)$ and IO which led to a rapid loss of IO (via the O + IO and IO + IO reactions) in their system. Due to the lack of details about their experiments, it is difficult to speculate further. We do not understand why Watson et al. [12] were unable to observe LIF of IO from the O + CF_3I reaction.

2.2. Kinetics of reactions (1) and (2)

The kinetics of reactions (1) and (2) were studied by measuring the temporal profiles of IO. The temporal profiles were obtained by varying the time delay between the photolysis and probe lasers between 10 μs and 70 ms. For all of these studies, IO was excited at ≈ 445 nm, the band head of the (2, 0) band. To determine the temperature dependence of the rate coefficients, a jacketed reaction cell was used. Fluids from a temperature controlled reservoir were flowed through the jacket. The temperature of the gas flowing through the reactor in the reaction zone was measured by inserting a thermocouple probe.

$I + O_3 \rightarrow IO + O_2$, ($k_1$). I atoms were generated by the 351 nm photolysis of CH_2I_2 in an excess of O_3. In all experiments, $[CH_2I_2]$ and $[O_3]$ were maintained such that the O atoms produced by O_3 photolysis were < 20 times that of the initial I atoms generated via CH_2I_2 photolysis. Therefore, the formation of IO from the reaction of O atoms with CH_2I_2 was negligible. O_2 was added to rapidly quench any electronically excited iodine atoms ($^2I_{1/2}$) that were possibly produced,

$$^2I_{1/2} + O_2 \rightarrow {}^2I_{3/2} + O_2(^1\Delta), \tag{6}$$

(k_6(298 K) = 4×10^{-11} cm^3 $molecule^{-1}$ s^{-1}) [24] before it reacted with ozone. O_2 also scavenged the CH_2I photoproduct, which otherwise could react with O_3 and, possibly, produce IO.

$$CH_2I + O_2 \overset{M}{\rightarrow} CH_2IOO, \tag{7}$$

$$CH_2I + O_3 \rightarrow CH_2O + IO + O_2. \tag{8}$$

Typically, CH_2I_2 ((4–16) $\times 10^{13}$ molecule cm^{-3}) was photolyzed at 351 nm (E = 3–16 mJ cm^{-2} $pulse^{-1}$) in the presence of excess O_3 ((1.3–32) $\times$ 10^{14} molecule cm^{-3}), N_2 (80 Torr) and O_2 (20 Torr). Preparation, storage, and handling of O_3 is discussed elsewhere [19]. The concentration of O_3 was measured in the main gas flow by UV absorbance at 253.7 nm ($\sigma_{O_3}^{253.7\,nm} = 1.16 \times 10^{-17}$ cm^2 $molecule^{-1}$) [17]. CH_2I_2 was maintained in a temperature controlled bubbler, through which a small flow N_2 was maintained. The CH_2I_2 concentration was measured by UV absorbance at 213.9 nm in a 10 cm long absorption cell ($\sigma_{CH_2I_2}^{213.9\,nm} = 3.2 \times 10^{-18}$ cm^2 $molecule^{-1}$) [25] and then added to the main gas flow just prior to entering the LIF reactor. The CH_2I_2 concentration was varied by changing the temperature of the bath (T = 255 to 277 K).

Following the photolytic production of I atoms, the temporal profile of IO is governed by

$$[IO]_t = \frac{k_1[I]_0[O_3]}{k_{10} - k'_a}\left[\exp(-k'_a t) - \exp(-k_{10}t)\right], \tag{9}$$

where we assume that the only product of reaction (1) is IO and k_{10} describes a first order loss process due to diffusion from the reaction zone and reactions with other species,

$$IO \rightarrow loss. \tag{10}$$

In Eq. (9), $k'_a = k_1[O_3] + k_{11}$, where process (11) represents an analogous loss process for I atoms,

$$I \rightarrow loss. \tag{11}$$

A typical temporal profile of IO when I atoms were produced in the presence of excess O_3 is shown in Fig. 2. The IO concentration increased exponentially and then decayed slowly. Such profiles were fit to Eq. (9) using a nonlinear least squares fitting routine to obtain k'_a. Temporal profiles were measured at various concentrations of O_3. A plot of the

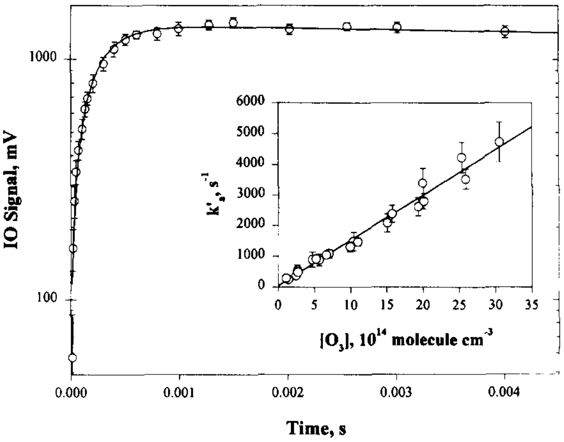

Fig. 2. Temporal profile of IO from the 351 nm photolysis of CH_2I_2 (4×10^{13} molecule cm^{-3}) and O_3 (2.5×10^{15} molecule cm^{-3}) in 80 Torr of N_2 and 20 Torr of O_2. The line is the nonlinear least squares fit to Eq. (9). The inset is a plot of k'_a versus $[O_3]$ at 298 K. The line is the linear least squares fit and yields the rate coefficient k_1 as the slope.

obtained values of k'_a versus $[O_3]$ is shown in the inset of Fig. 2. The slope of this plot gives the second order rate constant k_1. It should be noted that the loss of I atoms via process (11) was very small, $\approx 75\ s^{-1}$. Also the loss of IO was very slow (25–50 s^{-1}) and was probably due to diffusion and the IO + IO reaction. Even though the self reaction is second order in IO, it could be treated as a first order process for small losses of IO. Also there is no net loss of IO if the self reaction produces I atoms since IO would be regenerated by reaction (1). However, it could alter the IO temporal profile. Variation of the initial $[I]_0$ (either by changing $[CH_2I_2]$ or laser fluence) from $(2.5–13) \times 10^{11}$ molecule cm^{-3} did not affect the measured rate constant k_1, implying that IO + IO was not occurring to a significant extent during the course of reaction (1).

The rate coefficient, k_1, was measured at various temperatures and the results are shown in Table 1 and plotted in Arrhenius form in Fig. 3. A linear least squares analysis of ln k_1 versus 1/T gives: $k_1(T) = (2.3 \pm 0.7) \times 10^{-11} \exp[-(860 \pm 100)/T]$ cm^3 $molecule^{-1}$ s^{-1} over the temperature range $T = 240–370$ K. The error reported is 2σ and includes the precision and estimated systematic uncertainties due to measurement of the O_3 concentration at 298 K (5%) and temperature (1%).

IO + NO → I + NO₂, (k₂). To study reaction (2), IO ($\approx 3 \times 10^{11}$ molecule cm^{-3}) was produced via reaction (3) by photolyzing a mixture of N_2O (2×10^{15} molecule cm^{-3}), I_2 ($\approx 3 \times 10^{14}$ molecule cm^{-3}), and N_2 (5–100 Torr) at 193 nm (ArF laser, 1.8 mJ $pulse^{-1}$ cm^{-2}). Preparing, storing, and measuring of [NO] has been described elsewhere [19]. I_2 was added to the reactor by passing a small flow of N_2 over a trap containing solid I_2. Its concentration was measured after the LIF reactor by absorption ($\sigma_{I_2}^{508\ nm} = 2.5 \times 10^{-18}$ cm^2 $molecule^{-1}$) [26] using a Cd light source and a monochromator equipped with a photomultiplier tube. $O(^1D)$ produced by N_2O photolysis was rapidly quenched in < 0.5 μs by the large excess of N_2 and production of IO was complete within ≈ 100 μs. Although I_2 does photolyze at 193 nm [27], the I atoms produced did not affect the IO temporal profile. The temporal profile of IO obtained in such a system is shown in Fig. 4 (curve (a)). IO exhibited a fast exponential rise and then slowly decayed. Analysis of the IO appearance rate from profiles such as these gave a value for the rate coefficient for reaction (3) of $k_3 = (1.2 \pm 0.4) \times 10^{-10}$ cm^3 $molecule^{-1}$ s^{-1} at 298 K in agreement with literature values [16,17].

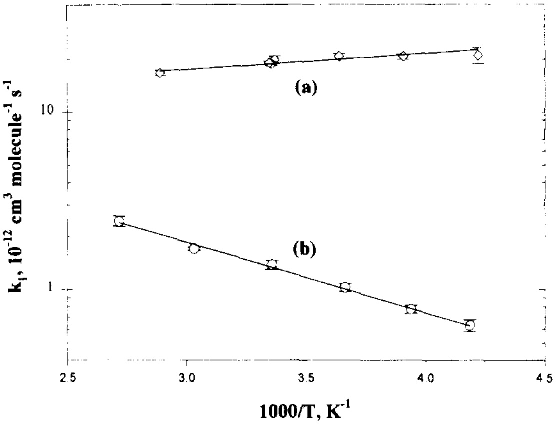

Fig. 3. Plot showing the variation of (a) k_2 and (b) k_1 with temperature. The line is the least squares fit to the Arrhenius expression: $k(T) = A\exp(-E_a/RT)$.

Table 1
Summary of the rate coefficients for reaction (1)

Temperature (K)	$[O_3]$ (10^{14} molecule cm^{-3})	$[I]_0$ (10^{11} molecule cm^{-3})	$k_1 \pm 2\sigma$ [a] (10^{-12} cm^3 $molecule^{-1}$ s^{-1})
239	3.1–34.0	5.0	0.63 ± 0.05
254	1.6–25.8	5.0	0.78 ± 0.04
273	1.8–27.6	5.0	1.03 ± 0.05
298	1.4–30.6	2.7–13	1.38 ± 0.08
331	1.2–20.0	5.0	1.70 ± 0.03
368	1.2–10.4	5.0	2.43 ± 0.16

[a] σ is the precision of the k' versus $[O_3]$ plot only.

When NO was added, the long time decay of IO increased substantially (see Fig. 4, curve (b)), whereas the appearance of IO was unaffected. In the presence of NO, the IO temporal profile can be described by

$$[IO]_t = \frac{k'_b[O]_0}{k'_d - k'_b}\left[\exp(-k'_b t) - \exp(-k'_d t)\right], \quad (12)$$

where $k'_b = k_3[I_2]$ and $k'_d = k_2[NO] + k_{10}$. In the majority of our experiments, production of IO was much faster than the loss via reactions (2) and (10). In this case the temporal profile of IO, after it reaches the maximum, is given by

$$[IO]_t = [IO]_0 \exp(-k'_d t). \quad (13)$$

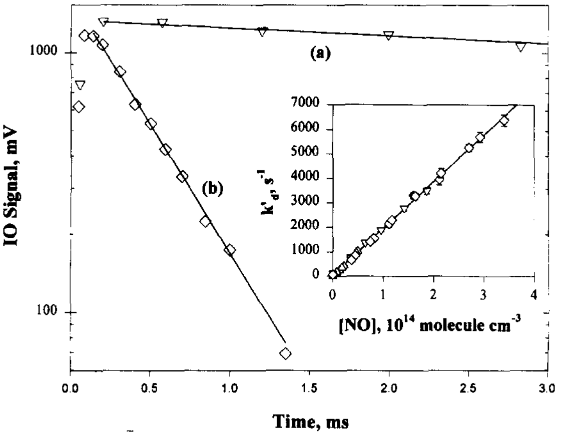

Fig. 4. IO temporal profiles from the 193 nm photolysis of N_2O (2×10^{15} molecule cm^{-3}) and I_2 (4×10^{14} molecule cm^{-3}) with (a) [NO] = 0 and (b) [NO] = 1.2×10^{14} molecule cm^{-3}. The lines are the least squares fits to Eq. (12). The inset is a plot of k'_d versus [NO] at 298 K. The total pressure was: △, 6 Torr, ▽, 23 Torr, and ◇, 100 Torr of N_2. The line is the linear least squares fit and yields the rate coefficient k_2 as the slope.

The long time decays of IO were typically fit to Eq. (13) to determine k'_d. However, at the highest NO concentrations and the lowest temperatures used, loss due to reaction (2) was competitive with IO formation. Here, the low vapor pressure of I_2 limited its concentration to $< 1 \times 10^{14}$ molecule cm^{-3}. In this case the IO temporal profiles were fit to Eq. (12) to determine k'_d. A plot of the k'_d versus [NO] at 298 K is shown in the inset of Fig. 4. The slope of this line yields the value of k_2. Such measurements were carried out at various temperatures between 237 and 347 K to obtain the values of k_2 listed in Table 2 and shown in Fig. 3. This data can be expressed as: $k_2(T) = (1.02 \pm 0.31) \times 10^{-11} \exp[(185 \pm 70)/T]$ cm^3 $molecule^{-1}$ s^{-1}. The errors are 2σ and include estimated systematic uncertainties in the [NO] (≈ 8%) and temperature (1%).

Table 2
Summary of the rate coefficients for reaction (2)

Temperature (K)	P_{tot} (Torr)	[NO] (10^{14} molecule cm^{-3})	$k_2 \pm 2\sigma$ [a] (10^{-11} cm^3 $molecule^{-1}$ s^{-1})
237	100	0.34–3.67	2.09 ± 0.21
256	100	0.37–3.92	2.07 ± 0.07
275	100	0.46–3.85	2.07 ± 0.08
298	5	0.06–0.50	1.98 ± 0.09
298	23	0.35–1.9	1.87 ± 0.04
298	100	0.36–3.41	1.90 ± 0.05
346	100	0.29–3.43	1.66 ± 0.06

[a] σ is the precision of the k' versus [NO] plot only.

3. Discussion

3.1. LIF of IO

The major finding of this work is that IO can be detected very easily using LIF. It is interesting to note that we could detect fluorescence from all the low lying bands except the one leading to $IO(A^2\Pi_{3/2}, v' = 1)$. This suggests that the $v' = 1$ state may dissociative more rapidly than the $v' = 0$, 2, or 3 states. We could not detect fluorescence from the (2, 2) band, which is consistent with very little population in the $v'' = 2$ level at 298 K. Measurement of the dispersed fluorescence spectra from these bands and the lifetimes of the various states would be useful in assessing the nature of the upper state in IO. Such information would also be valuable for optimizing IO detection via LIF.

The detection limit for IO at the (2, 0) band head was typically $\approx 1 \times 10^9$ molecule cm^{-3}. The noise was determined by the scattered light from the probe laser. We did not attempt to minimize this noise because the sensitivity was sufficient for our purposes. However, in an optimized system, this noise could be reduced by at least an order of magnitude. Also, we used a very broad excitation source, i.e. not all the probe energy was useful in exciting fluorescence. If one were to match the line width of the laser to that of IO and tune on and off the sharp lines, the sensitivity for detecting IO can be improved further. We estimate that suitable improvements could allow one to possibly detect $\approx 1 \times 10^6$ molecule cm^{-3} of IO. Recent modeling studies [11] suggest that this level of sensitivity would be adequate for detecting IO in the atmosphere.

3.2. Reaction (1)

The measured value of k_1 was independent of the variations in parameters such as pressure (30–200 Torr), $[I]_0$, $[CH_2I_2]$ and photolysis laser fluence. This invariance suggests that our measured value of

k_1 was not affected by any secondary reactions. The major uncertainties in the measured value of k_1 were due to the precision of the measurements in the temporal profiles, fitting of the profiles to Eq. (9), and the uncertainties in the concentration of O_3. We estimate the systematic error in measuring the concentration of O_3 to be $\approx 5\%$.

Reaction (1) was first studied by Clyne and Cruse [28], who monitored the IO $A^2\Pi_{3/2}(v=4) \leftarrow X^2\Pi_{3/2}(v=0)$ transition as a function of time in a discharge-flow system. They deduced that about a third of the nascent IO was formed in the $v''=1$ state. Under the low pressure conditions of their experiment, vibrational quenching would not be as rapid as in the present high pressure study. Clyne and Cruse estimated their measured value $k_1(293\ \text{K}) = 8.3 \times 10^{-13}$ cm^3 molecule^{-1} s^{-1} to be uncertain by nearly a factor of two. Thus their value is consistent with that measured here. Jenkin and Cox [29] used a molecular modulation technique to derive $k_1(298\ \text{K}) = (9.6 \pm 3.0) \times 10^{-13}$ cm^3 molecule^{-1} s^{-1}, and Sander [26] used flash photolysis of I_2/O_3 to determine $k_1 = (9.5 \pm 1.5) \times 10^{-13}$ cm^3 molecule^{-1} s^{-1}. Both of these studies used UV absorption of the (4, 0) band to monitor [IO]. Although slightly lower than our current study, these measurements are in reasonable agreement with the room temperature value determined here. Only Buben et al. [30] have measured k_1 as a function of temperature (231–337 K) and report $k_1(T) = (2.30 \pm 0.2) \times 10^{-11} \exp[-(880 \pm 30)/T]$ cm^3 molecule^{-1} s^{-1} using a discharge flow system with resonance fluorescence detection of I atoms. This measurement is in excellent agreement with the value determined in the present experiment. Using the data of Sander, Jenkin and Cox, Buben et al., and this study, we recommend $k_1(298\ \text{K}) = 1.2 \times 10^{-12}$ cm^3 molecule^{-1} s^{-1}, $A = (2.3 \pm 0.7) \times 10^{-11}$ cm^3 molecule^{-1} s^{-1}, $E/R = 870 \pm 100$ K^{-1}. In the format used in current data evaluations [16,17] the uncertainty factor for $k(298\ \text{K})$ is $f(298\ \text{K}) = 1.2$ and $\Delta E/R = \pm 100$.

3.3. Reaction (2)

As in the case of the reaction (1), the measured values of k_2 were insensitive to variations in the experimental parameters such as photolysis fluence ($E = 1.2$–2.4 mJ pulse^{-1} cm^{-2}), pressure (5–100 Torr), $[N_2O]$ (1–4×10^{15} molecule cm^{-3}) and $[I_2]$ (1–4.5×10^{14} molecule cm^{-3}). Therefore, we are confident that our measured values of k_2 were not significantly affected by any systematic errors. Ray and Watson [31] measured $k_2(298\ \text{K}) = (1.67 \pm 0.16) \times 10^{-11}$ cm^3 molecule^{-1} s^{-1} using a discharge flow–mass spectrometry system at 1–2 Torr. Inoue et al. [14] detected IO by LIF and report $k_2 = (2.8 \pm 0.2) \times 10^{-11}$ cm^3 molecule^{-1} s^{-1} at 298 K. In a comprehensive study, Daykin and Wine [32] used pulsed laser photolysis to produce IO and long path absorption to detect IO and reported $k_2(T) = (6.9 \pm 1.7) \times 10^{-12} \exp[(328 \pm 71)/T]$ cm^3 molecule^{-1} s^{-1} and $k_2(298\ \text{K}) = 2.1 \times 10^{-11}$ cm^3 molecule^{-1} s^{-1}, independent of pressure. The unpublished results of Buben et al. [33] yield $k_2(T) = (1.03 \pm 0.09) \times 10^{-11} \exp[(210 \pm 80)/T]$ cm^3 molecule^{-1} s^{-1} and $k_2(298\ \text{K}) = 2.1 \times 10^{-11}$ cm^3 molecule^{-1} s^{-1}. The results of all of these studies are in very good agreement with our values, with the exception of Inoue et al., who report a $\approx 30\%$ higher value at 298 K. Using the results from all these studies we recommend $k_2(298\ \text{K}) = 2.0 \times 10^{-11}$ cm^3 molecule^{-1} s^{-1}, $A = (9.1 \pm 2.0) \times 10^{-12}$ cm^3 molecule^{-1} s^{-1}, $E/R = -240 \pm 100$. For data evaluations, uncertainty factors of $f(298\ \text{K}) = 1.1$ and $\Delta E/R = \pm 100$ are recommended.

Acknowledgements

This work was funded in part by NOAA's Climate and Global Change program and in part by NASA's Mission to Planet Earth program. The authors would like to thank S.B. Barone for his assistance during the initial stages of this work.

References

[1] J.L. Moyers and R.A. Duce, J. Geophys. Res. 77 (1972) 5229.

[2] J.E. Lovelock, R.J. Maggs and R.J. Wade, Nature 241 (1973) 194.

[3] W. Reifenhauser and K.G. Heumann, Atmos. Environ. 26A (1992) 2905.

[4] S. Klick and K. Abrahamsson, J. Geophys. Res. 97 (1992) 12683.

[5] O.C. Zafiriou, J. Geophys. Res. 79 (1974) 2730.

[6] W.L. Chameides and D.D. Davis, J. Geophys. Res. 85 (1980) 7383.

[7] M.E. Jenkin, R.A. Cox and D.E. Candeland, J. Atmos. Chem. 2 (1985) 359.

[8] E.P. Daykin and P.H. Wine, J. Geophys. Res. 95 (1990) 18547.

[9] R.B. Chatfield and P.J. Crutzen, J. Geophys. Res. 95 (1990) 22319.

[10] W.T. Sturges and L.A. Barrie, Atmos. Environ. 22 (1988) 1179.

[11] S. Solomon, R.R. Garcia and A.R. Ravishankara, J. Geophys. Res. 99 (1994) 20491.

[12] T.A. Watson, M. Addison and C. Wittig, Chem. Phys. Letters 78 (1983) 57.

[13] B.C.L. Kwong and R.S. Tse, J. Phys. Chem. 98 (1994) 823.

[14] G. Inoue, M. Suzuki and N.J. Washida, Phys. Chem. 79 (1983) 4730.

[15] J.P. Bekooy, W.L. Meerts and A. Dymanus, J. Mol. Spectry. 102 (1983) 320.

[16] R. Atkinson, D.L. Baulch, R.A. Cox, R.F. Hampson, J.A. Kerr and J. Troe, J. Phys. Chem. Ref. Data 21 (1992) 1125.

[17] W.B. DeMore, S.P. Sander, D.M. Golden, R.F. Hampson, M.J. Kurylo, C.J. Howard, A.R. Ravishankara, C.E. Kolb and M.J. Molina, Chemical kinetics and photochemical data for use in stratospheric modeling, JPL Publication 94-26 (Jet Propulsion Laboratory, Pasadena, 1994).

[18] G.L. Vaghjiani and A.R. Ravishankara, J. Phys. Chem. 93 (1989) 1948.

[19] A.A. Turnipseed, S.B. Barone and A.R. Ravishankara, J. Phys. Chem. 97 (1993) 5926.

[20] S.B. Barone, A.A. Turnipseed and A.R. Ravishankara, J. Phys. Chem. 98 (1994) 4602.

[21] M.K. Gilles, A.A. Turnipseed, Y. Rudich, R. Talukdar, P. Villata, L.G. Huey, J.B. Burkholder and A.R. Ravishankara, in preparation.

[22] R.A. Durie and D.A. Ramsey, Can. J. Phys. 36 (1958) 35.

[23] M.L.P. Rao, D.V.K. Rao and P.T. Rao, Phys. Letters 50A (1974) 341.

[24] D.H. Burde, T.T. Yang and R.A. McFarlane, Chem. Phys. Letters 205 (1993) 69.

[25] J.B. Burkholder, unpublished data.

[26] S.P. Sander, J. Phys. Chem. 90 (1986) 2194.

[27] J.A. Myer and J.A.R. Samson, J. Chem. Phys. 52 (1970) 716.

[28] M.A.A. Clyne and H.W. Cruse, Trans. Faraday Soc. 66 (1970) 2214.

[29] M.E. Jenkin and R.A. Cox, J. Phys. Chem. 89 (1985) 192.

[30] S.N. Buben, I.K. Larin, N.A. Messineva and E.M. Trofimova, Soviet J. Chem. Phys. 8 (1991) 200.

[31] G.W. Ray and R.T. Watson, J. Phys. Chem. 85 (1981) 2955.

[32] E.P. Daykin and P.H. Wine, J. Phys. Chem. 94 (1990) 4528.

[33] S.N. Buben, I.K. Larin, N.A. Messineva and E.M. Trofimova, (1994), to be published.